Available online at www.sciencedirect.com

SCIENCE DIRECT®

Journal of Molecular Catalysis A: Chemical 207 (2004) 163–171

JOURNAL OF MOLECULAR CATALYSIS A: CHEMICAL

www.elsevier.com/locate/molcata

Oxidation of ethylbenzene over "neat" and zeolite-Y-encapsulated copper tri- and tetraaza macrocyclic complexes

T.H. Bennur, D. Srinivas*, S. Sivasanker

Catalysis Division, National Chemical Laboratory, Pune 411 008, India

Received 12 April 2003; received in revised form 9 June 2003; accepted 18 June 2003

Abstract

Copper tri- and tetraaza macrocyclic complexes were synthesized, encapsulated in zeolite-Y and characterized. The "neat" and encapsulated complexes exhibited good catalytic activity in the oxidation of ethylbenzene at 333 K, using *tert*-butyl hydroperoxide as the oxidant. Acetophenone was the major product though small amounts of *o*- and *p*-hydroxyacetophenones were also formed revealing that C–H bond activation takes place both at benzylic and aromatic ring carbon atoms. Ring hydroxylation was more over the "neat" complexes than over the encapsulated complexes. The differences in selectivity are attributed to the formation of different types of "active" copper–oxygen intermediates, such as side-on peroxide, bis-μ-oxo complexes and Cu-hydroperoxo species, in different proportions over the "neat" and encapsulated complexes.

Keywords: Zeolite-encapsulated complexes; Cu-peraza macrocycles; Ethylbenzene oxidation; Ring hydroxylation; Benzylic oxidation; Copper–oxygen complexes; *tert*-Butyl hydroperoxide oxidation

1. Introduction

Transition metal peraza macrocyclic complexes have been widely investigated from the point of view of their stability, structure, spectroscopy and magnetic properties [1–7]. The macrocyclic ring imparts unusual properties to the metal complexes. For example, (i) the ligand field strength of a number of macrocyclic complexes is unusually high [1,3], (ii) the metal complexes are highly inert to dissociation (compared to metal–amine complexes) in acid solutions, and (iii) Rh(III) and Cr(III) complexes of 1,4,8,11-tetraazacyclotetradecane ([14]ane-N_4; cyclam) exhibit unusual photo-behavior [8,9]. Hage et al. [10] reported that the manganese complexes of 1,4,7-trimethyl-1,4,7-triazacyclononane (Me_3[9]ane-N_3; Me_3tacn) are highly effective catalysts for the bleaching of stains using H_2O_2 at low temperatures. These Mn complexes also exhibited remarkable catalytic activity in the presence of carboxylate buffers in the stereo-selective epoxidation of olefins and oxidation of alkanes and alcohols with H_2O_2, at ambient temperatures [11–18]. Compared to the Mn complexes, the catalytic activity of Cu-peraza macrocycles in selective oxidations is not explored much. It is known that the copper complexes of substituted tacn exhibit high activity in the oxidative polymerization of phenols [19–23]. The copper complexes of N,N',N''-triallyl-1,4,7-triazacyclononane activate CO_2 and lead to reductive coupling to form C–C bonds [24]. Silica bound Cu(II)-tacn catalyzes the hydrolysis of phosphodiesters [25].

Here, we report studies on "neat" and zeolite-Y-encapsulated Cu complexes of 1,4,7-triazacyclononane ([9]ane-N_3; tacn), 1,4,7-trimethyl-1,4,7-triazacyclononane, 1,4,7,10-tetraazacyclododecane ([12]ane-N_4; cyclen), 1,4,7,10-tetramethyl-1,4,7,10-tetraazacyclododecane (Me_4[12]ane-N_4; Me_4cyclen) and 1,4,8,11-tetraazacyclotetradecane, of varying ring size (Scheme 1). These complexes are characterized by elemental analysis, surface area, FT-IR, UV-Vis and EPR techniques. Their catalytic activities in the oxidation of ethylbenzene using *tert*-butyl hydroperoxide (TBHP) are evaluated. The influence of the size of the macrocyclic ring, substitution and zeolite-encapsulation on the structure, spectral properties and catalytic activities are analyzed.

---

[*] Corresponding author. Tel.: +91-20-5893761; fax: +91-20-5893761.
E-mail address: srinivas@cata.ncl.res.in (D. Srinivas).

1381-1169/$ – see front matter © 2003 Elsevier B.V. All rights reserved.
doi:10.1016/S1381-1169(03)00502-8

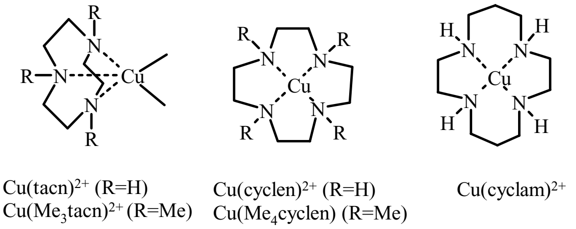

Scheme 1. Molecular structures of copper tri- and tetraaza complexes.

2. Experimental

2.1. Materials and catalyst preparation

2.1.1. Preparation of macrocyclic ligands

The macrocycles can be synthesized either in a “free” form [26] or bound to a given metal ion [27]. In the present work, the “free” ligands were prepared first and then complexed with Cu(II) ions. All the H-forms of the ligands were prepared by a modified Richmann–Atkin’s synthesis [28] and methylated as per the procedure reported for cyclam [29]. The present method of synthesis is a simplified procedure and applicable to all the peraza macrocycles used in this work. Schematic representation of the preparation of tacn, cyclen and their methylated compounds is shown in Scheme 2 and of cyclam is shown in Scheme 3.

Cyclization could be achieved by different routes (see Schemes 2 and 3) [28,30–34]. But the yields of the cyclized product varied with the route (Table 1). Cyclization using diol-ditosylates [28,33,34] (Table 1; see route 3 for Ts-tacn and route 1 for Ts-cyclen) was found to be more efficient than the halide routes [30–32].

Detosylation is a crucial step in the synthesis of cyclic peraza ligands as it had to be carried out under drastic conditions that can sometimes lead to ring opening. Among the various methods, detosylation using sulfuric acid [28] was found to be superior. The cyclic amine was precipitated as its sulfate salt from the acidic mixture by the addition of ethanol/ether. In the sulfuric acid method, high yields of **5a** and **5b** were obtained by minimizing water. *N*-Methylation of **5a** and **5b** with formic acid and formaldehyde afforded **6a** and **6b** in high yields. In the case of cyclam, the tosylation step yielded **9** in good yields. However, the yields in the detosylation step were very low (24%).

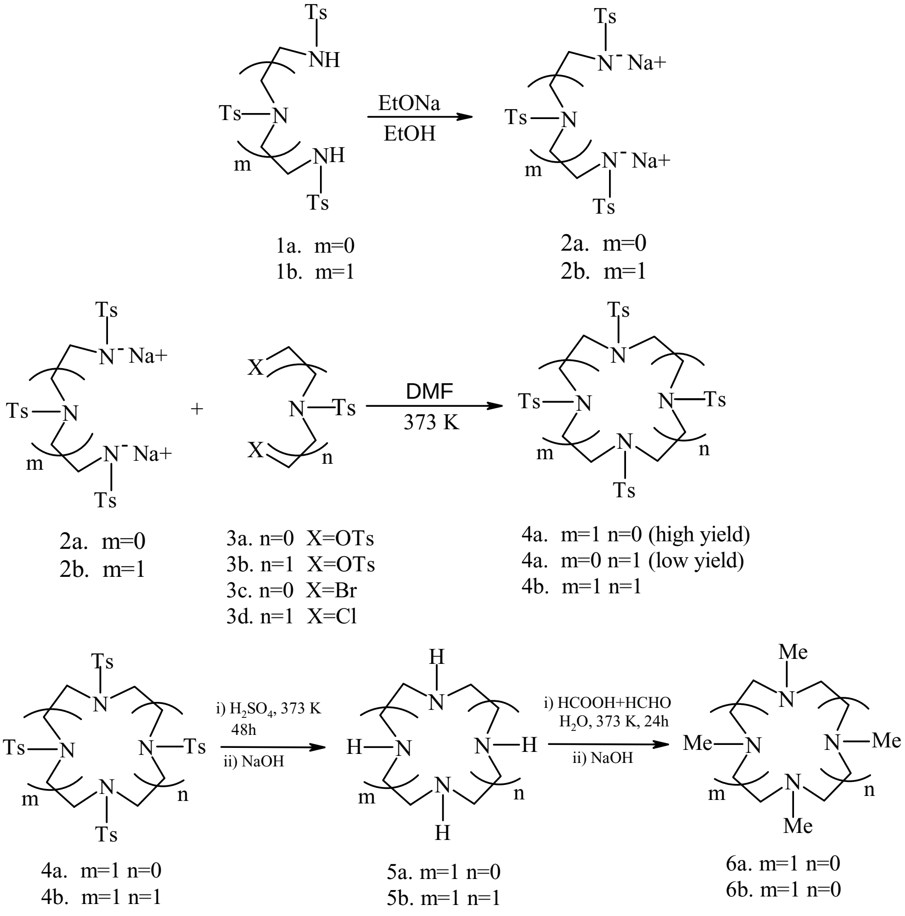

Scheme 2. Synthetic methodology of tacn and cyclen and their *N*-methylated derivatives.

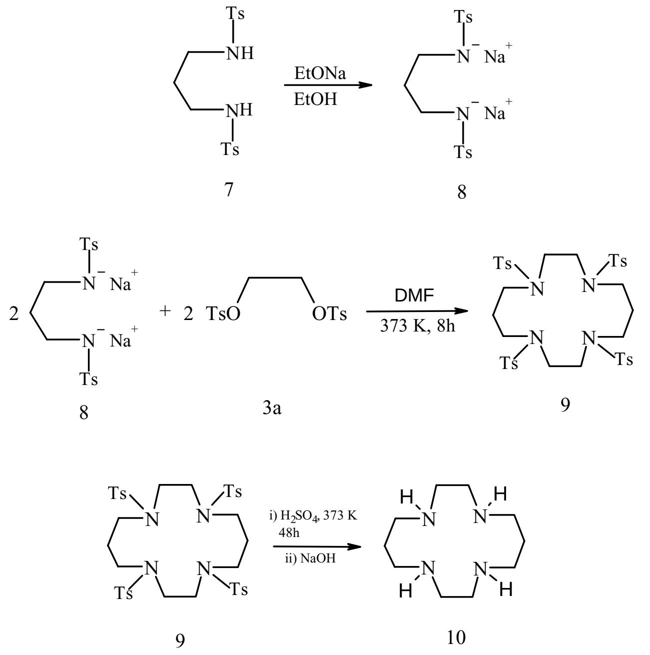

Scheme 3. Synthetic methodology of cyclam.

Purity of the ligands was confirmed by FT-NMR, IR and mass spectroscopy. The characterization data of different ligands (given below) agree well with the literature values [35–38].

2.1.1.1. 1,4,7-Triazacyclononane (tacn). ^{1}H NMR ($CDCl_3$; δ ppm): 2.79 (s, 6H), 2.63 (br, 3H); IR (Nujol, cm^{-1}): 3306, 2854–2928, 1660, 1458, 1364, 1157, 1032, 997; MS: $M^{\bullet+}$ 126, 112, 99, 85, 73, 56, 44 (base peak).

2.1.1.2. 1,4,7-Trimethyl-1,4,7-triazacyclononane (Me$_3$tacn). ^{1}H NMR ($CDCl_3$; δ ppm): 2.38 (s, 9H), 2.70 (s, 12H); IR (Nujol, cm^{-1}): 2802–2900, 1666, 1600, 1454, 1373, 1290, 1076, 1031, 999; MS: $M^{\bullet+}$ 171, 154, 147, 127, 115, 99, 84, 70, 58, 42 (base peak).

2.1.1.3. 1,4,7,10-Tetraazacyclononane (cyclen). ^{1}H NMR ($CDCl_3$; δ ppm): 2.68 (s, 16H), 2.39 (br, 4H); IR (Nujol, cm^{-1}): 3280, 2852–2924, 1560, 1462, 1350, 1110, 941, 759; MS: $M^{\bullet+}$ 170, 153, 136, 121, 104, 85, 80, 56, 44 (base peak).

2.1.1.4. 1,4,7,10-Tetramethyl-1,4,7,10-tetraazacyclodecane (Me$_4$cyclen). ^{1}H NMR ($CDCl_3$; δ ppm): 2.49 (s, 12H), 2.79 (s, 16H); IR (Nujol, cm^{-1}): 2941–2848, 1598, 1462, 1365, 1195, 1118, 1070, 1029, 923, 729; MS: $M^{\bullet+}$ 228, 213, 199, 186, 169, 149, 124, 113, 99, 82, 70, 58, 42 (base peak).

2.1.1.5. 1,4,8,11-Tetrazacyclotetradecane (cyclam). ^{1}H NMR ($CDCl_3$; δ ppm): 1.75 (m, 4H), 2.16 (s, 8H), 2.93 (m, 8H); IR (Nujol, cm^{-1}): 3276, 3192, 2854–2960, 1468, 1370, 1205, 1126, 1070, 830.

2.1.2. Preparation of “neat” Cu(II) complexes

2.1.2.1. Cu(tacn)(ClO_4)$_2$·2CH_3OH. The copper complexes were prepared by a modified procedure of Chaudhuri et al [39]. Methanolic solution (3 ml) of $CuCl_2\cdot 4H_2O$ (1 mmol, 0.17 g) and $NaClO_4$ (1.5 mmol, 0.198 g) were added simultaneously to tacn (1 mmol, 0.13 g) in methanol (3 ml). The solution was stirred for 1 h at 298 K and then heated at 333 K for another 1 h. The green precipitate was filtered and washed with cold methanol. All the manipulations were done under Ar atmosphere. Yield—49% (0.230 g).

The copper complexes of Me$_3$tacn, cyclen, Me$_4$cyclen and cyclam were prepared in a similar manner using $CuCl_2\cdot 2H_2O$/$Cu(CH_3COO)_2\cdot H_2O$.

2.1.3. Preparation of zeolite-Y-encapsulated metal complexes

Cu-exchanged NaY was prepared first by exchanging NaY (2 g) with Cu^{2+} ions from an aqueous solution (10 ml) of copper acetate (0.024 g). The slurry was stirred for 12 h. The solid was filtered and washed repeatedly with distilled water. Cu-Y, thus obtained by the ion exchange method, was dried at 393 K for 12 h. The amount of Cu-loading was found to be 0.25 wt.% (by AAS).

Cu-Y (2 g) was mixed with the corresponding peraza macrocyclic ligand in methanol (ligand:metal = 4:1). The solvent was then evaporated and the mixture was further heated in a glass reactor under nitrogen atmosphere, at

Table 1
Product yields in various cyclizations leading to tosylated tacn and tosylated cyclen

Tosylated cyclic amine[a]	Reactants[a]		Reaction time (h)	Yield (%)
	Disodium salt	Coupling agent		
Ts-tacn—route 1 (**4a**)	**2a**	**3d**	12	47
Ts-tacn—route 2 (**4a**)	**2b**	**3c**	14	64
Ts-tacn—route 3 (**4a**)	**2b**	**3a**	6	96
Ts-tacn—route 4 (**4a**)	**2a**	**3b**	8	55
Ts-cyclen—route 1 (**4b**)	**2b**	**3b**	7	89
Ts-cyclen—route 2 (**4b**)	**2b**	**3d**	16	59

[a] See Scheme 2 for description of the synthesis routes and the codes.

373 K, for 1 h. The temperature was slowly raised to 473 K, and maintained for 6 h. It was then cooled, and the unreacted ligand and loosely bound complex (at the external surface) were removed by Soxhlet extraction, initially with acetonitrile and then, with acetone for 8–10 h. The catalyst was dried at 383 K for 5 h.

2.2. *Physicochemical measurements*

The metal content was estimated using atomic absorption spectroscopy (AAS; Varian Spectrophotometer SF-220) and C, H and N content was determined on a Carlo Erba EA 1108 elemental analyzer. The surface area measurements were done by nitrogen adsorption/desorption at 77 K, using a Coulter (Omnisorb 100 CX) instrument. The FT-IR spectra of the "neat" complexes (as Nujol mulls) and encapsulated samples (in reflectance mode) were recorded on a Shimadzu 8201 PC spectrophotometer in the region, 400–4000 cm^{-1}. The UV-Vis spectra of the "neat" (in normal absorption mode) and encapsulated complexes (in diffuse reflectance mode) were measured on a Shimadzu UV-2550 spectrophotometer in the region of 200–800 nm. The EPR spectra (at 298 and 77 K) were recorded on a Bruker EMX spectrometer operating at X-band frequency and 100 kHz field modulation. The spectral simulations and manipulations were done using the Bruker Simfonia and WINEPR software packages, respectively.

2.3. *Catalytic activity studies and product analysis*

The catalytic activity runs were conducted in a 25 ml glass round bottom flask placed in a thermostated oil bath and fitted with a water cooled condenser. In a typical oxidation, ethylbenzene (0.106 g; 1 mmol), catalyst (0.004 mmol—in case of "neat" complexes and 0.02 g—in case of encapsulated complexes), TBHP (50% in ethylene dichloride; 0.42 ml) and CH_3CN (1 ml) were taken and the reaction was conducted at 333 K for 10 h. The progress of the reaction was monitored by GC (Varian 3400; CP-SIL8CB column; 30 m × 0.53 mm) and the products were identified by GC–MS (Shimadzu QP 5000; DB 1 column; 30 m × 0.25 mm) and GC–IR (Perkin-Elmer 2000; BP-1 column; 25 m × 0.32 mm).

3. Results and discussion

3.1. *Catalyst characterization*

The copper complexes of tacn and Me_3tacn were green, while that of cyclen and Me_4cyclen were blue and of cyclam were red. The color of the complexes changed upon encapsulation in zeolite-Y possibly due to molecular isolation, intermolecular interactions being negligible in the encapsulated complexes (vide infra). Chemical composition (Table 2) confirmed the formation and purity of the complexes. It is estimated from the elemental analysis that the complex molecules occupy one in every four supercages of zeolite-Y.

Surface area (S_{BET}) of the encapsulated complexes decreased systematically with an increase in the molecular dimensions of the macrocyclic ligand (Table 2). S_{BET} decreased from 540 m^2/g (for Cu-Y) to 498 m^2/g for Cu(tacn)-Y, 485 m^2/g for Cu(cyclen)-Y and 405 m^2/g for Cu(cyclam)-Y. The surface area decreased further on methyl substitution (Table 2).

Representative FT-IR spectra of the "neat" and encapsulated tacn, cyclen and cyclam complexes are shown in Fig. 1 (left and right panels, respectively). The "neat" complexes showed peaks at 3150–3280 and 2850–2980 cm^{-1} characteristic of N–H and C–H stretching vibrations, respectively. The vibrations due to C–N and C–C were observed at around 1251 and 1076 cm^{-1}, respectively (Table 3). In the encapsulated complexes, the O–H bands of zeolite-Y and adsorbed water masked the bands of the ligands.

Table 2
Physicochemical data of cyclic tri- and tetraaza Cu(II) complexes

Catalyst	Color	Chemical analysis (%)[a]					S_{BET} (m^2/g)
		C	H	N	C/N	Cu[a]	
$Cu(tacn)(ClO_4)_2 \cdot 2CH_3CN$	Green	25.4 (25.3)	4.7 (4.4)	13.8 (14.8)	1.7 (1.7)		
$Cu(Me_3tacn)(ClO_4)_2$	Green	35.9 (35.7)	6.9 (6.9)	12.8 (13.8)	2.8 (2.8)		
$Cu(cyclen)(ClO_4)_2 \cdot 2CH_3OH$	Blue	24.2 (24.0)	6.6 (5.7)	11.3 (11.2)	2.2 (2.1)		
$Cu(Me_4cyclen)(ClO_4)_2$	Blue	28.3 (29.3)	6.3 (5.7)	11.0 (11.4)	2.5 (2.5)		
$Cu(cyclam)(ClO_4)_2$	Red	26.2 (25.9)	5.2 (5.2)	11.8 (12.1)	2.2 (2.1)		
Cu(tacn)-Y	Pale brown	4.2	1.5	2.0	2.1 (1.7)	0.59	498
$Cu(Me_3tacn)$-Y	Pale green	3.8	1.9	1.5	2.5 (2.8)	0.65	490
Cu(cyclen)-Y	Green	5.4	2.4	2.2	2.4 (2.1)	0.77	485
$Cu(Me_4cyclen)$-Y	Blue	3.2	2.0	1.0	3.1 (2.5)	0.76	460
Cu(cyclam)-Y	Pink	2.7	2.1	1.0	2.7 (2.1)	0.82	405
Cu-Y	Pale blue	–	–	–	–	0.96	540

[a] Theoretical values are given in parentheses.

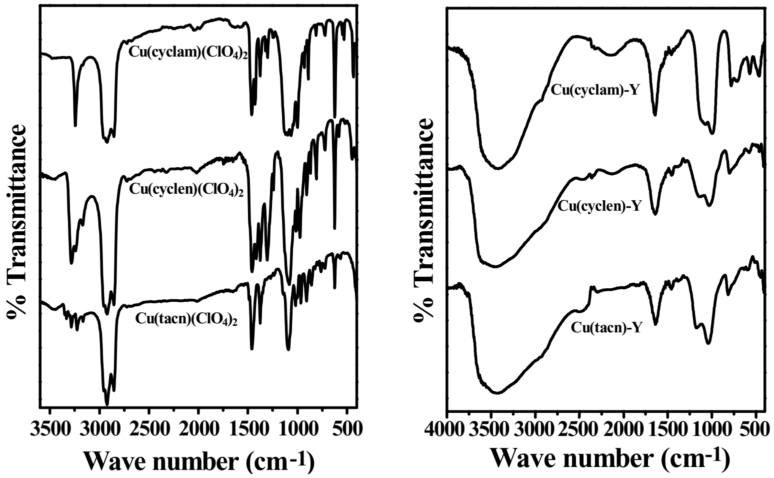

Fig. 1. FT-IR spectra of “neat” and zeolite-Y-encapsulated Cu(II)-tacn, cyclen and cyclam complexes.

Fig. 2 shows the UV-Vis spectra of “neat” and zeolite-Y-encapsulated complexes. The “neat” complexes in acetonitrile showed a characteristic UV band of ligand origin in the region 250–300 nm. A weak band due to metal-centered d–d transitions was observed in the visible range at 450–800 nm (Fig. 2, left panel). The size of the macrocyclic ligand affected the structure. As a consequence of this, the d–d band shifted from 660 nm in $Cu(tacn)^{2+}$ to 505 nm in $Cu(cyclam)^{2+}$ (Fig. 2, left panel, see inset). The ligand-centered band also shifted from 273 nm in $Cu(tacn)^{2+}$ to 255 nm in $Cu(cyclam)^{2+}$. This shift in the band position to the higher energy side indicates that the tetraaza ligand (cyclam) provides higher stability than the triaza ligand and the ligand field is stronger in cyclam than in tacn complexes. When the complexes were encapsulated in zeolite-Y, again the d–d band shifted to the higher energy side (by 15 nm in cyclam and 20 nm in tacn complexes) (Fig. 2; right panel). The stability of the complexes apparently increases when they are encapsulated in zeolite-Y. The position of the d–d band corresponds to a square pyramidal geometry for $Cu(tacn)^{2+}$ and a square planar geometry for both $Cu(cyclen)^{2+}$ and $Cu(cyclam)^{2+}$ [40].

$Cu(cyclam)^{2+}$ in CH_3CN showed a EPR spectrum at 77 K characteristic of axial symmetry. Hyperfine features due to copper were resolved in the parallel region. The spectrum of the encapsulated complex was almost similar to that of the frozen solution (Fig. 3) confirming the formation of molecules inside the zeolite cages and indicating their isolation. Polycrystals of “neat” $Cu(cyclam)^{2+}$ did not show such resolved copper hyperfine features (Fig. 3) due to the intermolecular interactions that were obviously avoided in frozen solutions and also in the encapsulated complexes. The similarity in EPR spectra of frozen solution and encapsulated $Cu(cyclam)^{2+}$ complexes further reveals that the geometry of the complex does not change significantly upon encapsulation.

Fig. 4 shows the EPR spectra of copper exchanged Y and the encapsulated complexes. CuY showed a spectrum characterized by spin Hamiltonian parameters of $g_\parallel = 2.395$,

Table 3
Spectroscopic data of cyclic tri- and tetraaza Cu(II) complexes

Catalyst	FT-IR data (cm^{-1})			UV-Vis (nm)	EPR data[a]		
	ν(C–N)	ν(C–C)	ν(N–H)		$g_\parallel$	$g_\perp$	$A_\parallel$ (G)
$Cu(tacn)(ClO_4)_2\cdot 2CH_3CN$	1232	1076	3284	660	2.046 (2.288)	2.165, 2.105 (2.098)	NR (155.5, 35.0)
$Cu(Me_3tacn)(ClO_4)_2$	1251, 1298	1074	–	608	(2.245)	(2.045)	(170.0, 13.0)
$Cu(cyclen)(ClO_4)_2\cdot 2CH_3OH$	1244	1078	3240	600	2.130 (2.192)	2.060 (2.068)	NR (170.0, 13.0)
$Cu(Me_4cyclen)(ClO_4)_2$	1278, 1294	1078	–	590	2.179 (2.200)	2.063 (2.095)	NR (182.4, 10.0)
$Cu(cyclam)(ClO_4)_2$	1299	1064	3242	505	2.160 (2.180)	2.048 (2.081)	NR (207.0, 25.0)
Cu(tacn)-Y				640	2.229	2.056	166.9
$Cu(Me_3tacn)$-Y				600	2.305	2.067	148.4
Cu(cyclen)-Y				600	2.205	2.057	180.4
$Cu(Me_4cyclen)$-Y				490, 640	2.207	2.063	173.7
Cu(cyclam)-Y				490	2.178	2.047	202.0
Cu-Y				480, 600	2.395	2.083	126.4

[a] Values for frozen methanolic solutions (77 K) are given in parentheses.

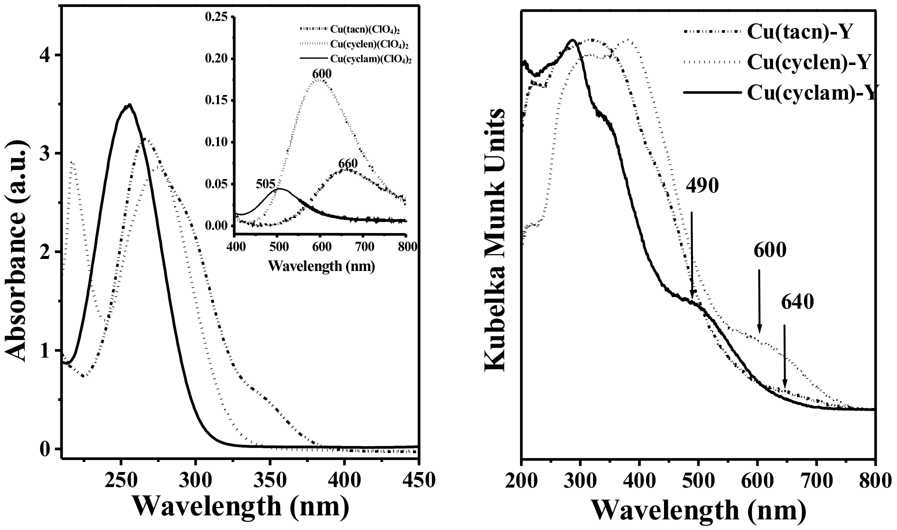

Fig. 2. UV-Vis spectra of "neat" and zeolite-Y-encapsulated Cu(II)-tacn, cyclen and cyclam complexes.

$g_\perp = 2.083$ and $A_\parallel(\mathrm{Cu}) = 126.4\,\mathrm{G}$. These signals due to exchanged Cu ions were absent in the spectra of encapsulated Me$_3$tacn, cyclen, Me$_4$cyclen and cyclam indicating that nearly all the exchanged Cu(II) ions formed the complexes. A small quantity of uncomplexed Cu(II) ions were noticed in Cu(tacn)-Y. Spectral simulations revealed considerable change in the g and A(Cu) parameters of the different Cu complexes (Table 3). The spectrum of Cu(cyclam)$^{2+}$ corresponds to that of a square planar complex and that of Cu(cyclen)$^{2+}$ and Cu(Me$_4$cyclen)$^{2+}$ are attributable to weakly pentacoordinated structures. The high $g_\parallel$ and low $A_\parallel$ values of Cu(tacn)$^{2+}$ and Cu(Me$_3$tacn)$^{2+}$ indicate square pyramidal geometry and depletion of electron density at the site of Cu(II). The latter can happen if the geometry is distorted and Cu is out of the basal plane. X-ray structures of Cu(tacn)Cl$_2$ [41] and Cu(tacn)Br$_2$ [42] reveal a distorted square pyramidal geometry wherein the cyclic triamine occupies two equatorial sites and one axial site. The Cu atom is raised by about 0.2 Å from the basal plane toward the axial nitrogen atom. Such a distortion in the geometry can lead to

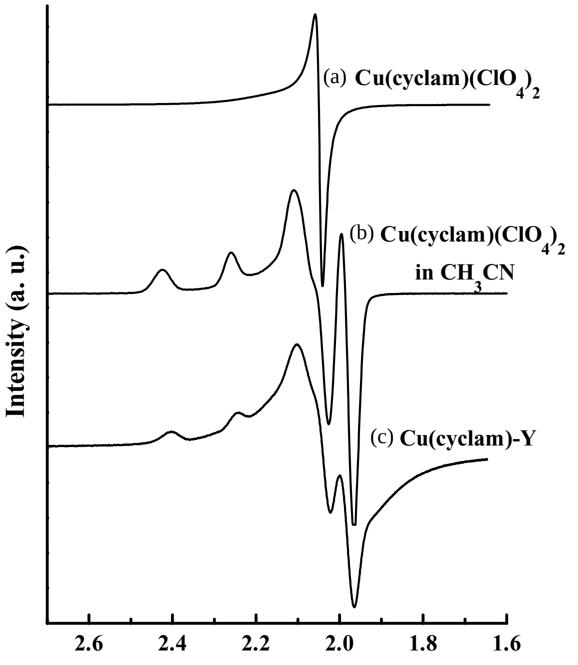

Fig. 3. EPR spectra of Cu(cyclam)(ClO$_4$)$_2$ at 100 K: (a) polycrystals, (b) frozen CH$_3$CN solution and (c) zeolite-Y-encapsulated complexes.

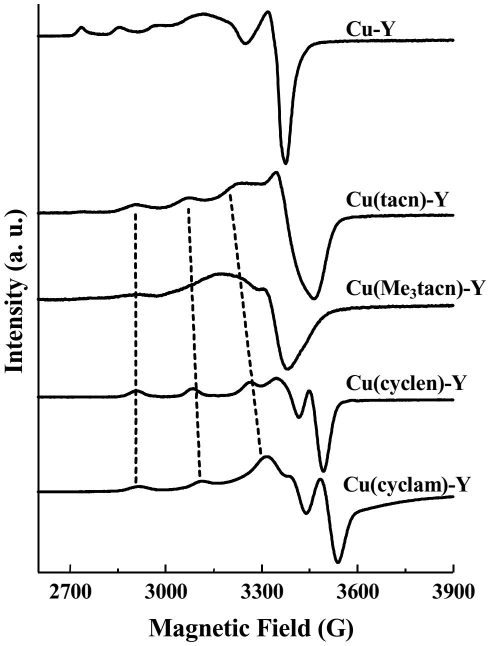

Fig. 4. EPR spectra of Cu-Y and encapsulated peraza macrocyclic complexes at 298 K.

low hyperfine coupling parameters. The shift in the d–d band position (Fig. 2) also agrees with this change in the molecular geometry. No major changes in the EPR parameters were observed when the complexes are encapsulated in the cages of zeolite-Y, again revealing that the structure of the complexes is not changed due to encapsulation. Chemical composition reveals the formation of mono-ligand complexes. Bis–ligand complexes, for example, $Cu(tacn)_2{}^{2+}$ are supposed to possess C_{3v} or D_{3h} geometry and exhibit an isotropic EPR signal at ambient temperatures due to Jahn-Teller effect. Absence of such an EPR signal rules out the formation of bis–ligand complexes both in solutions and in the zeolite.

3.2. *Oxidation of ethylbenzene*

The peraza macrocyclic complexes exhibited good activity in the oxidation of ethylbenzene using TBHP (Table 4). The reaction did not proceed in the absence of metal complexes. Also, no reaction occurred when aqueous H_2O_2 was used in place of TBHP, as the oxidant. Acetophenone (AcPh) is the major product; *o*-/*p*-hydroxyacetophenones and other products such as benzaldehyde are also formed in small quantities (Table 4). The type of the macrocyclic ring and encapsulation affected the activity and product selectivity. Turnover frequency (TOF, h^{-1}) for complexes with different ligands decreased in the order: tacn > cyclam > Me_4cyclen > cyclen (for “neat” complexes) and tacn > cyclam > cyclen > Me_4cyclen (for the encapsulated complexes). The encapsulated complexes exhibited higher activity (TOF) than the “neat” complexes. Aromatic ring hydroxylation was more with “neat” tetraaza macrocyclic complexes than with the triaza complex; it decreased in the order: Me_4cyclen > cyclen > cyclam > tacn. Cu-Y exhibited high catalytic activity (TOF = 87.2 h^{-1}) but the selectivity for acetophenone was lower than that of the encapsulated complexes (Table 4).

Aromatic ring hydroxylation was less when the reactions were conducted using the encapsulated complexes (Table 4). The encapsulated complexes showed enhanced selectivity for AcPh. The extent of selectivity enhancement (for AcPH) is more in the case of tetraaza complexes (13–16%) than with the triaza complex (6%). This difference in the catalytic activity/selectivity of the peraza complexes in the “neat” form and when encapsulated in zeolites is probably due to the formation of different “active” copper–oxygen complexes.

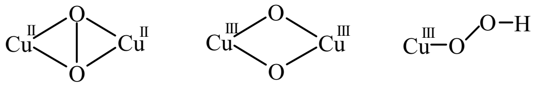
Side-on peroxo-Cu_2^{II} Bis-(μ-oxo)-Cu_2^{III} Hydroperoxo-Cu_2^{II}

Scheme 4. Structures of copper–oxygen species.

At least three types of “active” Cu–O_2 species, viz. side-on peroxo-$Cu_2{}^{II}$ ($\mu - \eta^2, \eta^2$), bis-μ-oxo-$Cu_2{}^{III}$ and mononuclear Cu^{II}-hydroperoxide (Scheme 4) have been identified in the binding, activation and reduction of oxygen to water by copper proteins [43]. Tyrosinase, a dinuclear copper protein, catalyzes the aromatic ring hydroxylation involving dimeric Cu-species such as side-on peroxo-$Cu_2{}^{II}$ and probably, bis-μ-oxo-$Cu_2{}^{III}$ intermediates. Dopamine β-monooxygenase that catalyzes side chain hydroxylation forms a mononuclear Cu(II)-hydroperoxo intermediate [43]. Such types of oxo intermediates are formed in the present system also. Side-on peroxo-$Cu_2{}^{II}$ and bis-μ-oxo-Cu_2 dimers (responsible for ring hydroxylation) are the more feasible forms in homogeneous solutions with the “neat” complexes. In fact, bis-μ-oxo-Cu_2-tacn complexes were isolated from the homogeneous oxygenated solutions and structurally characterized [44]. The possibility of forming such dimers is less likely in the case of encapsulated complexes as the individual molecules are well separated and confined to the cavities. Thus, a significant suppression in ring hydroxylated products is observed in catalysis by the encapsulated complexes. Steric effects, weak electrostatic interactions and the synergism due to interactions with

Table 4
Catalytic activity data in the oxidation of ethylbenzene with tri- and tetraaza Cu(II) complexes[a]

Catalyst[b]	Time (h)	Conversion (mol%)	TOF (h^{-1})	Selectivity (mol%)		
				AcPh	*o*-/*p*-Hydroxy AcPh	Others[c]
$Cu(tacn)(ClO_4)_2$	10	49.6	24.8	91.0	3.7	5.3
Cu(tacn)-Y (0.15%)	10	37.0	77.9	97.0	2.9	0.1
$Cu(cyclen)(ClO_4)_2$	8	19.0	6.0	64.2	8.0	27.8
Cu(cyclen)-Y (0.20%)	10	30.5	48.5	80.2	4.3	15.5
$Cu(Me_4cyclen)(ClO_4)_2$	10	35.1	8.8	71.0	13.5	15.5
$Cu(Me_4cyclen)$-Y (0.20%)	10	27.8	44.0	85.9	6.3	7.8
$Cu(cyclam)(ClO_4)_2$	10	44.5	11.1	85.9	7.8	6.3
Cu(cyclam)-Y (0.21%)	10	44.4	67.0	98.0	2.0	–
Cu-Y (0.25%)	3	20.6	87.2	67.6	6.5	25.9

[a] Reaction conditions: ethylbenzene = 0.105 g (1 mmol); catalyst = 0.004 mmol (“neat” complex) or 0.02 g (encapsulated complex); 50% TBHP in ethylenedichloride = 0.42 ml; CH_3CN = 1 ml; temperature = 333 K.

[b] Metal content (wt.%) is given in parentheses.

[c] Others mainly include benzaldehyde.

the zeolite framework are the other possible reasons for the differences in the reactivity of the encapsulated complexes. When the reaction was conducted at 313 K instead of 333 K, higher amounts of aromatic ring hydroxylated products were formed and the selectivity for acetophenone was low indicating that the stability of the binuclear side-on peroxo complexes is higher at low temperatures (313 K).

Controlled UV-Vis and EPR experiments were performed to investigate the different “active” copper–oxygen species formed with the “neat” and encapsulated complexes upon contacting TBHP. Fig. 5(i) shows the UV-Vis spectra of “neat” Cu(tacn)(ClO$_4$)$_2$ complexes in acetonitrile before (curve a) and after interacting with TBHP (curve b). The complexes showed an absorption band attributable to d–d transitions at 650 nm. Upon contacting with TBHP a new band was observed at about 462 nm and the intensity of the d–d transition decreased (curve b). The new band at 462 nm is attributed to bis-μ-oxo dimeric complex. This band for related substituted tacn complexes [45] and for the binuclear Cu model system containing *N*,*N*,*N*′,*N*′-tetra(2-pyridylethyl)-3,5-di-(aminomethyl)phenyl [43] occurs at 430–448 nm. The characteristic charge transfer band due to Cu-hydroperoxide should appear at around 600 nm [43]. This band, supposed to be weak, could not be separated as it perhaps overlapped with the broad d–d band (curve b). EPR spectroscopy provided evidence for the formation of Cu-hydroperoxide species (Fig. 5(ii)). Significant changes in the spectra were observed upon contact with TBHP. In Cu(cyclam)$^{2+}$, the spectrum characterized by the signals with $g_{\parallel} = 2.187$, $g_{\perp} = 2.053$ and $A_{\parallel} = 202$ G due to the original complex (curve a) were replaced by the signals due to two new paramagnetic Cu(II) species I and II (curves b and c). Species I is characterized by $g_{\parallel} = 2.419$, $g_{\perp} = 2.081$ and $A_{\parallel} = 117$ G. Species II is characterized by $g_{\parallel} = 2.333$, $g_{\perp} = 2.081$ and $A_{\parallel} = 102$ G). The overall spectral intensity decreased indicating that part of the Cu ions formed diamagnetic side-on peroxo or μ-oxo type species. The new species formed upon contacting with TBHP are the Cu$^{\mathrm{II}}$-hydroperoxo species. Solomon et al. [43] reported based on detailed spectroscopic and theoretical studies that mononuclear copper(II) alkyl and hydroperoxo complexes show EPR spectrum with large g values and small hyperfine splitting features. Indeed the large $g_{\parallel}$ value (2.419 and 2.333) and small $A_{\parallel}$ values (117 and 102 G) for species I and II indicate the formation of Cu-hydroperoxide species. Thus, based on the combined UV-Vis and EPR spectroscopic studies it can be concluded that both copper-oxo and hydroperoxo species are formed in the interaction of copper tri- and tetraaza complexes with TBHP. The difference in their relative concentration is presumably responsible for the difference in the selectivity behavior.

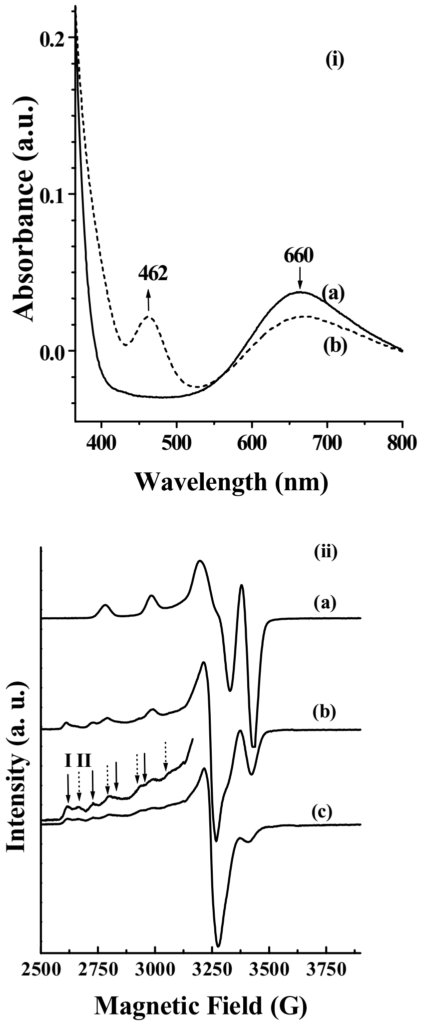

Fig. 5. (i) UV-Vis spectra of Cu(tacn)(ClO$_4$)$_2$: (a) before and (b) after adding TBHP. (ii) EPR spectra of Cu(cyclam)(ClO$_4$)$_2$: (a) before, (b) after 4 h and (c) after 10 h of adding TBHP. Parallel hyperfine features due to Cu-hydroperoxide species I and II are marked.

4. Conclusions

The “neat” and zeolite-Y-encapsulated copper tri- and tetraaza macrocyclic complexes exhibit efficient catalytic activity in the regioselective oxidation of ethylbenzene using TBHP. C–H activation occurs at both the benzylic and aromatic ring carbon atoms. The latter is significant over the “neat” complexes in the homogeneous phase, while it is suppressed significantly in the case of the encapsulated complexes. The encapsulated complexes exhibit enhanced activity and selectivity in the oxidation reaction. Molecular isolation and the absence of intermolecular interactions (as revealed by EPR spectroscopy), synergism due to interaction with the zeolite framework and restricted access of the active site to ethylbenzene are the probable reasons for the differences in activity/selectivity of the encapsulated catalysts. The type of the “active” copper–oxygen species (side-on peroxide, bis-μ-oxo complex and Cu-hydroperoxide) formed during the reaction probably determines the product selectivity. The size of the macrocyclic ring and substitution also influence the catalytic activity.

Acknowledgements

D.S. acknowledges DST, New Delhi for financial support. T.H.B. thanks CSIR, New Delhi for the award of Senior Research Fellowship.

References

[1] P. Chaudhuri, K. Wieghardt, in: S.J. Lippard (Ed.), Progress in Inorganic Chemistry, vol. 35, Wiley, New York, 1987, p. 329.
[2] K.P. Wainwright, Coord. Chem. Rev. 166 (1997) 35.
[3] D.H. Busch, Acc. Chem. Res. 11 (1978) 392.
[4] K. Wieghardt, Angew. Chem. Int. Ed. Engl. 98 (1986) 1026.
[5] K. Wieghardt, Inorg. Chem. 22 (1983) 2953.
[6] M. Enomoto, T. Aida, J. Am. Chem. Soc. 124 (2002) 6099.
[7] C.N. Verani, E. Bothe, D. Burdinski, T. Weyhermuller, U. Florke, P. Chaudhuri, Eur. J. Inorg. Chem. (2001) 2161.
[8] D.B. Miller, P.K. Miller, N.A.P. Kane-Maguire, Inorg. Chem. 22 (1983) 3831.
[9] N.A.P. Kane-Maguire, W.S. Crippen, P.K. Miller, Inorg. Chem. 22 (1983) 696.
[10] R. Hage, J.E. Iburg, J. Kerschner, J.H. Koek, E.L.M. Lempers, R.J. Martens, U.S. Racherla, S.W. Russell, T. Swarthoff, M.R.P. van Vliet, J.B. Warnaar, L. van der Wolf, B. Krijnen, Nature 369 (1994) 637.
[11] B.F. Sels, A.L. Villa, D. Hoegaerts, D.E. De Vos, P.A. Jacobs, Topics Catal. 13 (2000) 223.
[12] D.E. De Vos, J.L. Meinershagen, T. Bein, Angew. Chem. Int. Ed. Engl. 35 (1996) 2211.
[13] Y.V. Subba Rao, D.E. De Vos, T. Bein, P.A. Jacobs, Chem. Commun. (1997) 355.
[14] D.E. De Vos, T. Bein, J. Am. Chem. Soc. 119 (1997) 9460.
[15] P.-P. Knops-Gerrits, D.E. De Vos, P.A. Jacobs, J. Mol. Catal. A: Chem. 117 (1997) 57.
[16] J.R.L. Smith, G.B. Shul'pin, Tetrahedron Lett. 39 (1998) 4909.
[17] G.B. Shul'pin, G. Süss-Fink, L.S. Shul'pina, J. Mol. Catal. A: Chem. 170 (2001) 17.
[18] T.H. Bennur, S. Sabne, S.S. Deshpande, D. Srinivas, S. Sivasanker, J. Mol. Catal. A: Chem. 185 (2002) 71.
[19] H. Higashimura, K. Fujisawa, Y. Moro-oka, M. Kubota, A. Shiga, A. Terahara, H. Uyama, S. Kobayashi, J. Am. Chem. Soc. 120 (1998) 8529.
[20] H. Higashimura, M. Kubota, A. Shiga, K. Fujisawa, Y. Moro-oka, H. Uyama, S. Kobayashi, Macromolecules 33 (2000) 1986.
[21] H. Higashimura, K. Fujisawa, S. Namekawa, M. Kubota, A. Shiga, Y. Moro-oka, H. Uyama, S. Kobayashi, J. Polym. Sci., Part A: Polym. Chem. 33 (2000) 4792.
[22] H. Higashimura, K. Fujisawa, Y. Moro-oka, M. Kubota, A. Shiga, H. Uyama, S. Kobayashi, J. Mol. Catal. A: Chem. 155 (2000) 201.
[23] K. Oyaizu, K. Saito, E. Tsuchida, Chem. Lett. (2000) 1318.
[24] L.J. Farrugia, S. Lopinski, P.A. Lovatt, R.D. Peacock, Inorg. Chem. 40 (2001) 558.
[25] B.R. Bodsgard, J.N. Burstyn, Chem. Commun. (2001) 647.
[26] C.K. Poon, M.L. Tobe, J. Chem. Soc. A (1968) 1549.
[27] E.K. Barefield, F. Wagner, A.W. Harlinger, A.R. Dahl, Inorg. Synth. 16 (1976) 220.
[28] J.E. Richmann, T.J. Atkins, J. Am. Chem. Soc. 96 (1974) 2268; J.E. Richmann, W.F. Orttle, Org. Synth. 58 (1978) 86.
[29] E.K. Barefield, F. Wagner, Inorg. Chem. 12 (1973) 2435.
[30] H. Koyama, T. Yashino, Bull. Chem. Soc. Jpn. 45 (1972) 481.
[31] L.Y. Martin, C.R. Sperati, D.H. Busch, J. Am. Chem. Soc. 99 (1977) 2968.
[32] R. Yang, J. Zompa, Inorg. Chem. 15 (1976) 1499.
[33] P.G. Graham, D.C. Weatherburn, Aust. J. Chem. 36 (1983) 2349.
[34] P.G. Graham, D.C. Weatherburn, Aust. J. Chem. 34 (1981) 291.
[35] C.J. Pouchert (Ed.), The Aldrich Library of NMR spectra, vol. 1, IInd ed., Aldrich, USA, 1983, pp. 588B, 590C.
[36] K. Wieghardt, P. Chaudhuri, H.-J. Nuber, Inorg. Chem. 21 (1982) 3086.
[37] G.R. Weisman, D.P. Reed, J. Org. Chem. 61 (1996) 5185.
[38] J.F. Desreux, E. Merciny, M.F. Loncin, Inorg. Chem. 20 (1981) 987.
[39] P. Chaudhuri, K. Oder, K. Wieghardt, B. Nuber, J. Weiss, Inorg. Chem. 25 (1986) 2818.
[40] B.J. Hathaway, in: Sir G. Wilkinson, G.D. Gillard, J.A. McCleverty (Eds.), Comprehensive Coordination Chemistry, vol. 5, Pergamon Press, Oxford, 1987, Chapter 53, p. 533.
[41] W.F. Schwindinger, T.G. Fawcett, R.A. Lalancette, J.A. Potenza, H.J. Schugar, Inorg. Chem. 19 (1980) 1379.
[42] R.D. Bereman, M.R. Churchill, P.M. Schaber, M.E. Winkler, Inorg. Chem. 18 (1979) 3122.
[43] E.I. Solomon, P. Chen, M. Metz, S.-K. Lee, A.E. Palmer, Angew. Chem. Int. Ed. 40 (2001) 4570.
[44] S. Mahapatra, J.A. Halfen, E.C. Wilkinson, G. Pan, X. Wang, V.G. Young Jr., C.J. Cramer, L. Que Jr., W.B. Tolman, J. Am. Chem. Soc. 118 (1996) 11555.
[45] K.D. Karlin, J.C. Hayes, Y. Gultneh, R.W. Cruse, J.W. McKnown, J.P. Hutchinson, J. Zubieta, J. Am. Chem. Soc. 106 (1984) 2121.